Xanthomonas oryzae pv. oryzae Type III Effector XopN Targets OsVOZ2 and a Putative Thiamine Synthase as a Virulence Factor in Rice

Hoon Cheong[1], Chi-Yeol Kim[2], Jong-Seong Jeon[2], Byoung-Moo Lee[3], Jae Sun Moon[4], Ingyu Hwang[1*]

1 Department of Agricultural Biotechnology, Seoul National University, Seoul, Korea, 2 Graduate School of Biotechnology & Crop Biotech Institute, Kyung Hee University, Yongin, Korea, 3 National Academy of Agricultural Science, Rural Development Administration, Suwon, Korea, 4 Plant Systems Engineering Research Center, Korea Research Institute of Bioscience and Biotechnology, Daejeon, Korea

Abstract

Xanthomonas oryzae pv. oryzae (Xoo) is spread systemically through the xylem tissue and causes bacterial blight in rice. We evaluated the roles of Xanthomonas outer proteins (Xop) in the Xoo strain KXO85 in a Japonica-type rice cultivar, Dongjin. Five xop gene knockout mutants ($xopQ_{KXO85}$, $xopX_{KXO85}$, $xopP1_{KXO85}$, $xopP2_{KXO85}$, and $xopN_{KXO85}$) were generated by EZ-Tn5 mutagenesis, and their virulence was assessed in 3-month-old rice leaves. Among these mutants, the $xopN_{KXO85}$ mutant appeared to be less virulent than the wild-type KXO85; however, the difference was not statistically significant. In contrast, the $xopN_{KXO85}$ mutant exhibited significantly less virulence in flag leaves after flowering than the wild-type KXO85. These observations indicate that the roles of Xop in Xoo virulence are dependent on leaf stage. We chose the xopN gene for further characterization because the $xopN_{KXO85}$ mutant showed the greatest influence on virulence. We confirmed that $XopN_{KXO85}$ is translocated into rice cells, and its gene expression is positively regulated by HrpX. Two rice proteins, OsVOZ2 and a putative thiamine synthase (OsXNP), were identified as targets of $XopN_{KXO85}$ by yeast two-hybrid screening. Interactions between $XopN_{KXO85}$ and OsVOZ2 and OsXNP were further confirmed in planta by bimolecular fluorescence complementation and in vivo pull-down assays. To investigate the roles of OsVOZ2 in interactions between rice and Xoo, we evaluated the virulence of the wild-type KXO85 and $xopN_{KXO85}$ mutant in the OsVOZ2 mutant line PFG_3A-07565 of Dongjin. The wild-type KXO85 and $xopN_{KXO85}$ mutant were significantly less virulent in the mutant rice line. These results indicate that $XopN_{KXO85}$ and OsVOZ2 play important roles both individually and together for Xoo virulence in rice.

Introduction

Xanthomonas oryzae pv. oryzae (Xoo) causes bacterial leaf blight, which is one of the most serious diseases in rice (Oryza sativa L.). This bacterium invades the xylem of rice leaves through hydathodes or wounds. The strain of Xoo KXO85 (KACC10331) was isolated from diseased rice leaves in Korea, and its whole genome sequence was published in 2005 [1].

Plant pathogenic bacteria belonging to the genera Pseudomonas, Xanthomonas, Erwinia, and Ralstonia possess the type III protein secretion system (T3SS) that is critical for full virulence and bacterial colonization in their host plants [2–6]. The T3SS of plant pathogenic species of Pseudomonas, Xanthomonas, Erwinia, and Ralstonia is highly conserved and involved in translocation of T3SS-dependent effector proteins from bacterial cells into plant cells [7–12]. These effector proteins are categorized into two groups: transcription activator-like (TAL) effectors and non-TAL effectors [11,13–15]. In Xoo, T3SS that is essential for virulence is encoded by hypersensitive response and pathogenicity (hrp) genes, the expression of which is controlled by HrpX [13,16,17].

T3SS-dependent plant bacterial effectors are important for bacterial growth, colonization, virulence, and race specificity in their host plants [18–23]. However, the biochemical functions of most T3SS-dependent plant bacterial effectors in their hosts have not been well characterized. Xanthomonas outer proteins (Xop) are known as non-TAL bacterial effector proteins that are delivered to the plant cell via Hrp T3SS. The major roles of non-TAL bacterial effectors involve modulation of signaling in the plant defense response [11,24]. For example, $XopX_{Xcv}$ from

X. campestris pv. *vesicatoria* (Xcv) affects the virulence of *Xcv* on pepper (*Capsicum annuum*) and tomato (*Lycopersicum esculentum*) and targets basic innate immunity in plants [24]. XopD$_{Xcv}$ is a small ubiquitin-like modifier (SUMO) protease in *Xcv* that promotes bacterial growth in tomato and slows leaf chlorosis and necrosis in tomato at late stages of infection [25]. Another T3SS-dependent non-TAL effector, XopN$_{Xcc}$, plays important roles in colonization and virulence of *X. campestris* pv. *campestris* (Xcc) in their hosts [26]. XopN is highly conserved among *Xanthomonas* species [27]. In addition, XopN$_{Xcv}$ may suppress pathogen-associated molecular pattern (PAMP)-triggered immunity in tomato [28].

Compared to known host targets of TAL effectors in xanthomonads, there have been few studies on non-TAL effector targets in xanthomonads. XopD$_{Xcv}$ may target nuclear SUMOylated proteins [25]. In *Xcc* and *Arabidopsis* interactions, XopD$_{XccB100}$ targets the transcription factor MYB30 to suppress host defense [29]. Recently, it was found that tomato transcription factor SlERF4 was identified as a target of XopD$_{Xcv}$ in tomato [30]. Non-TAL effector Xoo1488 of *Xoo* MAFF311018 targets two receptor-like cytoplasmic kinases (RLCKs), Os01g0936100 (OsRLCK55) and Os05g0372100 (OsRLCK185), to inhibit OsRLCK185 phosphorylation and the downstream MAPK signaling [31]. Other reported host targets of XopN$_{Xcv}$ are tomato atypical receptor-like kinase (TARK1) and four 14-3-3 isoforms (TFT1, TFT3, TFT5, and TFT6) [28].

In *Xoo*, considerable efforts have been made to characterize functional roles of TAL effectors in various strains [32,33]. The contribution of each TAL effector protein to *Xoo* virulence varies; some are critical for virulence, while others have relatively moderate roles [32,34]. However, the roles of non-TAL effectors in *Xoo* virulence have been poorly investigated. When 18 non-TAL effectors were evaluated for virulence in the Philippine strain PXO99^A, deletion of both copies of *xopZ$_{PXO99}$* conferred significant reduction of virulence, whereas the other non-TAL effectors showed little influence on virulence in 4-week-old rice leaves [35]. Disease severity of *Xoo* in susceptible cultivars varies depending on leaf stage [36–39]. This led us to assess the virulence of each *xop* mutant at the adult stage in the field with the expectation of more distinct and different disease response outcomes compared to virulence assay results at the young leaf stage. Here, we report the contribution of XopN$_{KXO85}$ to *Xoo* virulence in the Korean strain KXO85 at flag leaf stage in the field, identification of targets of XopN$_{KXO85}$ in rice, and their important roles for *Xoo* virulence.

Results

Mutagenesis of five *xop* genes in the Korean *Xoo* strain KXO85

Five *xop* genes, *xopQ$_{KXO85}$* (XOO4466), *xopX$_{KXO85}$* (XOO4287), *xopP1$_{KXO85}$* (XOO3425), *xopP2$_{KXO85}$* (XOO3426), and *xopN$_{KXO85}$* (XOO0343) (Table S1), were characterized among 18 *xop* homologs in the strain KXO85 (www.xanthomonas.org/t3e.html), which showed significant homology with reported *xop* genes. EZ-Tn5 insertion mutants of *xopQ$_{KXO85}$*, *xopX$_{KXO85}$*, *xopP1$_{KXO85}$*, *xopP2$_{KXO85}$*, and *xopN$_{KXO85}$* (Figure S1) were generated in the strain KXO85, and then the

virulence of each *xop* gene knockout mutant was evaluated in 3-month-old leaves of the Japonica-type rice cultivar Dongjin. Mutations in the *xopQ$_{KXO85}$*, *xopX$_{KXO85}$*, *xopP1$_{KXO85}$*, *xopP2$_{KXO85}$*, or *xopN$_{KXO85}$* gene did not significantly affect virulence (Figure 1A). When the *xopN$_{KXO85}$* mutant was inoculated into the flag leaves of Dongjin in the field, the mutant was significantly less virulent than the wild-type KXO85 (Figure 1B). Virulence the *xopN$_{KXO85}$* mutant carrying each wild-type *xop* gene in a multicopy plasmid was recovered to the wild-type level (Figure 1B). These observations indicate that *xopN$_{KXO85}$* exhibits important roles for virulence of *Xoo*. Therefore, we chose *xopN$_{KXO85}$* for further characterization. The bacterial population of the *xopN$_{KXO85}$* mutant was reduced up to 21 days after inoculation of flag leaves compared to the growth of wild-type strain KXO85 in Dongjin (Figure 1C).

### Expression of *xopN$_{KXO85}$* is regulated by HrpX$_{KXO85}$

As expression of *hrp* and *xop* genes in *Xcv* and other xanthomonads is controlled by two regulatory genes, *hrpG* and *hrpX*, we examined whether *xopN$_{KXO85}$* is regulated by HrpX$_{KXO85}$ in *Xoo* KXO85. Expression of *xopN$_{KXO85}$* was below the limit of detection as assessed by quantitative real-time polymerase chain reactions (PCR) in the wild-type KXO85 or in the *hrpX$_{KXO85}$* mutant strain in rich PSB medium (Figure S2A). In the *hrp*-inducing medium XOM2, *xopN$_{KXO85}$* expression in the wild-type KXO85 was approximately 3-fold higher than that in the *hrpX$_{KXO85}$* mutant (Figure S2A). We found a conserved *cis*-regulatory element plant-inducible promoter (PIP) box (TTCGG-N$_{15}$-TTCTG) in the region from -263 to -239 upstream of the start codon of *xopN$_{KXO85}$* (Figure S2B). These results indicate that *xopN$_{KXO85}$* belongs to the HrpX$_{KXO85}$ regulon in *Xoo* KXO85.

XopN$_{KXO85}$ is a T3SS-dependent effector translocated into plant cells in the strain KXO85

To investigate whether XopN$_{KXO85}$ is translocated into plant cells in a T3SS-dependent manner, we conducted a XopN$_{KXO85}$ translocation assay using the XopN-Cya fusion protein in the wild-type strain KXO85 and the T3SS-deficient mutant KXO85 *hrpB5$_{KXO85}$*::EZ-Tn5 in rice (Figure S3A). The level of cAMP increased in the wild-type strain KXO85, whereas no change in cAMP level was detected in the T3SS-deficient mutant KXO85 *hrpB5$_{KXO85}$*::EZ-Tn5 (Figure S3B). This indicates that XopN$_{KXO85}$ is translocated into rice cells in a T3SS-dependent manner.

Identification of XopN$_{KXO85}$ targets in rice by yeast two-hybrid screening

To identify XopN$_{KXO85}$ target proteins in rice, we carried out yeast two-hybrid screening using GAL4-XopN as a bait protein and a rice cDNA library constructed in the prey vector in the *Saccharomyces cerevisiae* strain MaV203. We found two possible candidates: *Oryza sativa* vascular plant one zinc finger protein 2 (OsVOZ2: NP_001056041, Os05g0515700) and *O. sativa* XopN$_{KXO85}$ binding protein (OsXNP: NP_001059841, Os07g0529600) (Figure 2A and Table S2). The *OsVOZ2* gene is 3,630 bp in length consisting of four exons and three introns and encodes a protein of 69,901 Da. OsVOZ2 is a homolog of *Arabidopsis thaliana* vascular plant
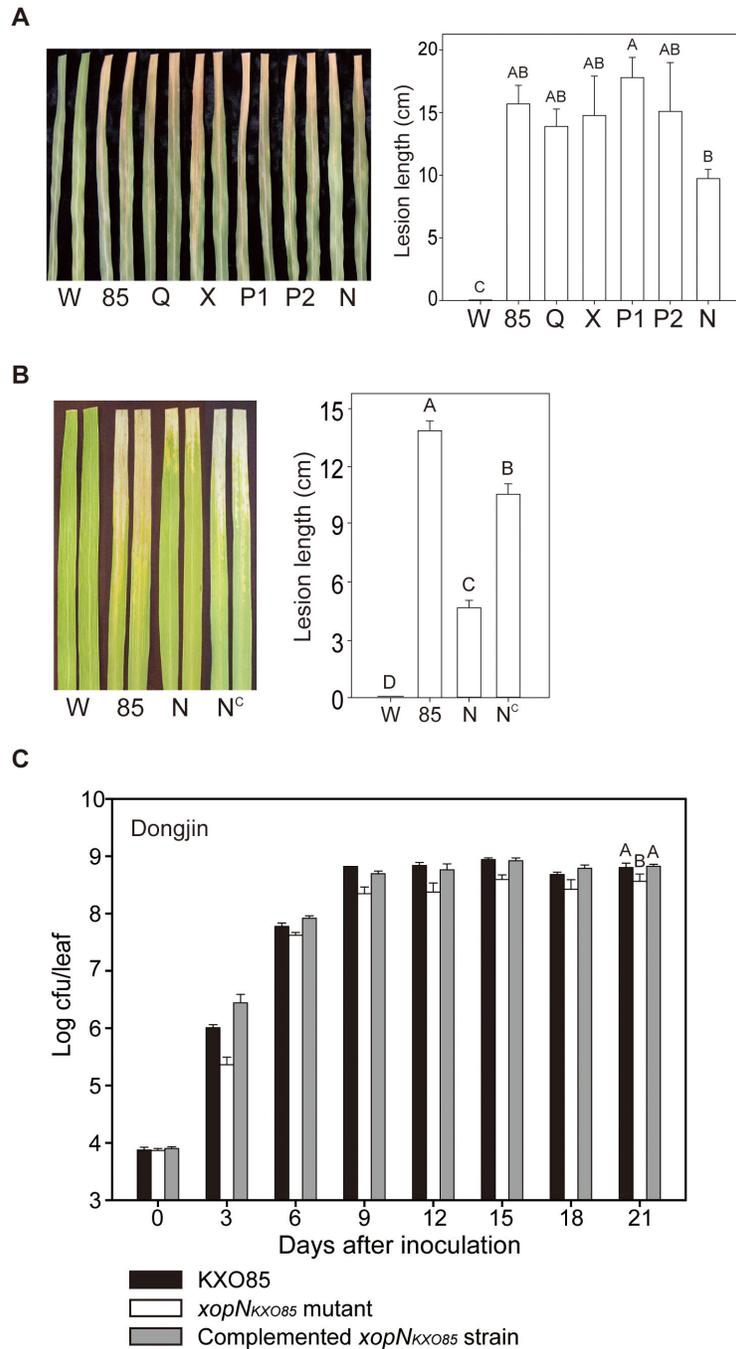
Figure 1. Pathogenicity test for *xop* mutants of *Xoo* KXO85 in rice. A. Disease severity of each *xop* mutant in 3-month-old rice leaves. W, water; 85, wild-type KXO85; Q, KXO85 *xopQ_{KXO85}*::EZ-Tn*5*; X, KXO85 *xopX_{KXO85}*::EZ-Tn*5*; P1, KXO85 *xopP1_{KXO85}*::EZ-Tn*5*; P2, KXO85 *xopP2_{KXO85}*::EZ-Tn*5*; N, KXO85 *xopN_{KXO85}*::EZ-Tn*5*. **B**. Disease severity of the *xopN_{KXO85}* mutants in the flag leaves of rice grown in a paddy field. W, water; 85, KXO85; N, KXO85 *xopN_{KXO85}*::EZ-Tn*5*; and N^C, KXO85 *xopN_{KXO85}*::EZ-Tn*5* (pML122G2). Photographs were taken and lesion lengths were determined 21 days after inoculation. Vertical error bars indicate the standard deviations (SD). The data are the averages of 12–15 replicates for each treatment. Columns and lines not connected by the same letter are significantly different (P<0.05) as determined by a one-way ANOVA (P<0.001) followed by post hoc Tukey HSD analysis. **C**. Bacterial growth patterns of the KXO85, *xopN_{KXO85}* mutant, and complemented *xopN_{KXO85}* mutant strains in flag leaves of wild-type Dongjin. The data are shown as the average values for three replicates; vertical bars indicate the error ranges (±SD). The bacterial populations were assessed every 3 days after inoculation. Different letters at day 21 indicate significant differences (P<0.05) as determined by a one-way ANOVA (P<0.001) followed by post hoc Tukey HSD analysis.

doi: 10.1371/journal.pone.0073346.g001
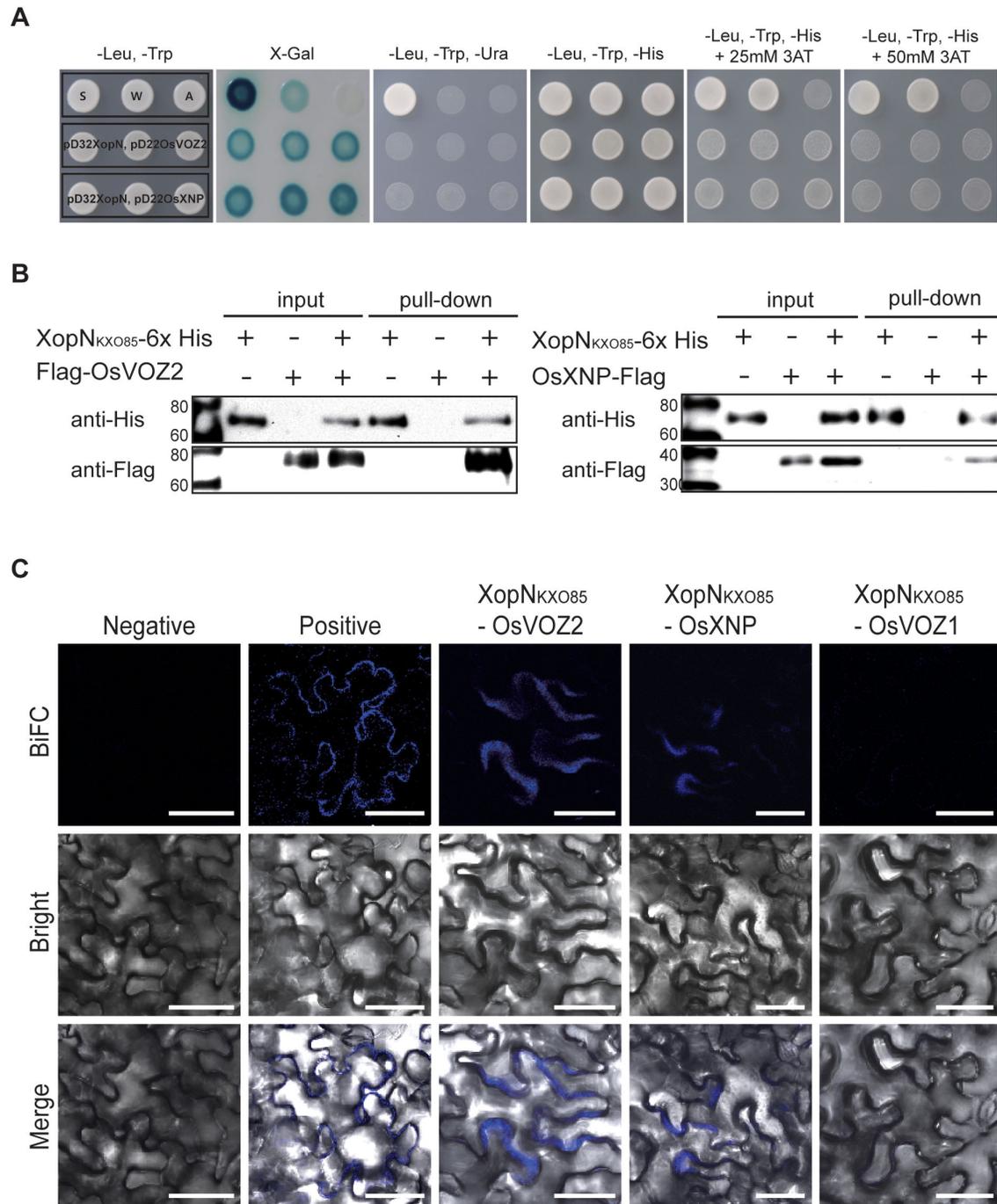
Figure 2. Interactions between XopN$_{KXO85}$ and OsVOZ2 and OsXNP. A. Screening for interactors of XopN$_{KXO85}$ in rice using a yeast two-hybrid system. S (strong: pEXP ™32/Krev1 + pEXP ™22/RalGDS-wt), W (weak: pEXP ™32/Krev1 + pEXP ™22/RalGDS-m1), and A (absent: pEXP ™32/Krev1 + pEXP ™22/RalGDS-m2) indicate the strength of each interaction. Three independent and representative colonies are shown for each bait–prey combination. **B**. *In vivo* pull-down analysis of XopN$_{KXO85}$ and OsVOZ2 (left panel) and XopN$_{KXO85}$ and OsXNP (right panel). Total proteins from *N. benthamiana* leaves co-expressing XopN$_{KXO85}$-6× His and Flag-OsVOZ2 or XopN$_{KXO85}$-6× His and OsXNP-Flag protein were purified by Ni$^+$ affinity chromatography followed by Western blotting using anti-His and anti-Flag antibodies. The expected molecular weights were as follows: XopN$_{KXO85}$-6× His = 78.7 kDa; Flag-OsVOZ2 = 74.6 kDa; OsXNP-Flag = 40.1 kDa; +, protein expressed; and -, vector control. **C**. BiFC analysis of XopN$_{KXO85}$ -OsVOZ2, XopN$_{KXO85}$ -OsXNP, and XopN$_{KXO85}$ -OsVOZ1 interactions in *N. benthamiana* leaves. Negative, pDEST-SCYNE(R)^{GW} + pDEST-SCYCE(R)^{GW}; positive, pEXP-SCYNE(R)-Cnx7 + pEXP-SCYCE(R)-Cnx6. Bars = 50 µm.

doi: 10.1371/journal.pone.0073346.g002

one zinc finger protein 2 (AtVOZ2; At2g42400) that has a conserved zinc finger domain (Figure S5 and Figure S6). The *OsXNP* gene is 1,489 bp in length with two exons and one intron and possibly encodes a putative protein of 37,224 Da that has significant homology with thiamine biosynthetic enzyme in *Saccharum* hybrid cultivar GT28 (Table S2). $XopN_{KXO85}$, OsVOZ2, and OsXNP were expressed in yeast as confirmed by immunoblot using anti-GAL4BD and anti-GAL4AD antibodies (Figure S4).

## $XopN_{KXO85}$ physically interacts with two rice proteins OsVOZ2 and OsXNP *in planta*

To confirm the specific interactions between $XopN_{KXO85}$ and OsVOZ2 and $XopN_{KXO85}$ and OsXNP *in planta*, we performed affinity pull-down experiments in *Nicotiana benthamiana* (*N. benthamiana*) leaves. Cells of *Agrobacterium tumefaciens* strain C58C1 (pCH32) carrying pGWB8-XopN (*xopN_{KXO85}*-6× His in pGWB8) or pGWB12-OsVOZ2 (Flag-*OsVOZ2* in pGWB12) were co-infiltrated into *N. benthamiana* leaves. For pull-down experiments to investigate interactions between $XopN_{KXO85}$ and OsXNP, *A. tumefaciens* cells harboring pGWB8-XopN and pGWB11-OsXNP (*OsXNP*-Flag in pGWB11) were co-infiltrated into *N. benthamiana* leaves. Eluted soluble proteins bound to Ni-nitrilotriacetic acid (Ni-NTA) superflow agarose slurry were subjected to immunoblotting analysis using anti-His or anti-Flag antibodies. Both Flag-OsVOZ2 and OsXNP-Flag proteins were pulled down by $XopN_{KXO85}$-6xHis (Figure 2B). These results indicate that $XopN_{KXO85}$ physically interacts with OsVOZ2 or OsXNP in *N. benthamiana* leaves.

Visualization of the interactions of OsVOZ2 and OsXNP with $XopN_{KXO85}$

A bimolecular fluorescence complementation (BiFC) assay was performed to examine the interactions between $XopN_{KXO85}$ and OsVOZ2 and $XopN_{KXO85}$ and OsXNP *in planta*. The coding sequences of *xopN_{KXO85}*, *OsVOZ2*, *OsXNP*, and *OsVOZ1* were cloned into pDEST-SCYNE(R)^GW and pDEST-SCYCE(R)^GW using the Gateway recombination system to yield pSCYNE(R)-XopN, pSCYCE(R)-OsVOZ2, pSCYCE(R)-OsXNP, and pSCYCE(R)-OsVOZ1, respectively (Table S3). When *Agrobacterium* cells carrying both plasmids were infiltrated into *N. benthamiana* leaves, the super cyan fluorescent protein (SCFP3A) signal was detected in the cytoplasm of the *N. benthamiana* cells (Figure 2C). As a positive control, we used the Cnx6 and Cnx7 interaction model to form a complex of molybdopterin synthase in *A. thaliana* using pEXP-SCYNE(R)-Cnx7 and pEXP-SCYCE(R)-Cnx6 [40]. These results indicate that $XopN_{KXO85}$ interacts with OsVOZ2 and OsXNP in the cytoplasm of *N. benthamiana* cells. However, $XopN_{KXO85}$ does not interact with OsVOZ1 in *N. benthamiana* cells (Figure 2C).

Subcellular localization of $XopN_{KXO85}$, OsVOZ2, and OsXNP

To determine their subcellular localizations, $XopN_{KXO85}$, OsVOZ2, and OSXNP were tagged with GFP at their C-termini in p2GWF7-XopN, p2GWF7-OsVOZ2, and p2GWF7-OsXNP, respectively (Table S3). In transient expression assays using maize mesophyll protoplasts, GFP signals from XopN-GFP and
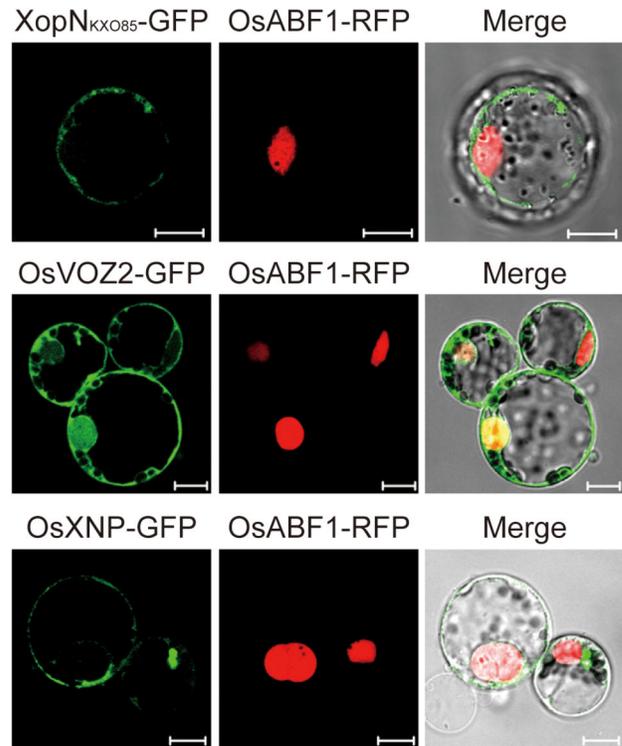
Figure 3. Localization of $XopN_{KXO85}$, OsVOZ2, and OsXNP in plant cells. Subcellular localization of the $XopN_{KXO85}$-GFP, OsVOZ2-GFP, and OsXNP-GFP fusion proteins in maize mesophyll cells. OsABF1-RFP was used as a nuclear marker. GFP (green) fluorescence was merged with RFP (red) fluorescence. Bars = 10 µm.

OsXNP-GFP were mostly detected in the cytoplasm, whereas those from OsVOZ2-GFP were detected in both the cytoplasm and the nucleus compared to the nuclear marker OsABF1-RFP (Figure 3). These data indicate that $XopN_{KXO85}$ and OsXNP are localized in the cytoplasm, whereas OsVOZ2 is localized in a nuclear and cytoplasm (Figure 3).

Interactions between $XopN_{KXO85}$ and OsVOZ2 are important for *Xoo* virulence in rice

To determine whether OsVOZ2 and its interactions with $XopN_{KXO85}$ are critical for *Xoo* virulence, the *OsVOZ2* knockout mutant line PFG_3A-07565 from the rice T-DNA Insertion Sequence Database (http://signal.salk.edu/cgi-bin/RiceGE) [41] was inoculated with wild-type KXO85. In the mutant line PFG_3A-07565, T-DNA is inserted 929 nucleotides downstream from the translational start site of *OsVOZ2*. RT-PCR analysis detected *OsVOZ2* transcript in wild-type Dongjin but not in the *OsVOZ2* mutant line PFG_3A-07565 (Figure 4A), which confirmed knockout mutation in *OsVOZ2*. Wild-type KXO85 and *xopN_{KXO85}* mutant strains were inoculated into wild-type Dongjin and the *OsVOZ2* mutant line, and the *xopN_{KXO85}* mutant was shown to exhibit reduced virulence in the wild-type Dongjin. However, both strains showed significantly reduced

disease severity in the *OsVOZ2* mutant line compared to the wild-type Dongjin (Figure 4B). The *xopN*$_{KXO85}$ mutant was less virulent in the *OsVOZ2* mutant line than the wild-type KXO85 (Figure 4B and 4C). The population of *xopN*$_{KXO85}$ mutant was smaller than that of wild-type KXO85 in the *OsVOZ2* mutant line (Figure 4D). These results indicate that XopN$_{KXO85}$ is a virulence factor and that its interactions with OsVOZ2 are critical for *Xoo* virulence in rice.

Discussion

There has been some confusion regarding the roles of Xop of *Xoo* because previous studies have used different *Xoo* strains. The *Xoo* PXO99^A strain has 18 non-TAL bacterial effectors [35]. Among these, XopZ$_{PXO99}$ acts as a virulence factor in the *Xoo* PXO99^A strain and suppresses plant basal defense mechanisms [35]. XopR$_{MAFF311018}$ was reported as a virulence factor in rice and inhibits the plant basal defense in *A. thaliana* [42]. Nine non-TAL effectors have been identified in the Chinese strain 13751, among which XopR$_{13751}$ has been shown to affect virulence in *Xoo* [43]. In the present study, we chose XopN$_{KXO85}$ to evaluate functional roles in the KXO85 strain and confirmed that it is secreted in an Hrp T3SS-dependent manner, translocated into the plant cytoplasm, and that its gene expression is regulated by HrpX$_{KXO85}$, as reported previously for other *Xoo* strains [13]. Among the Xop homologs in KXO85, we found that XopN$_{KXO85}$ is the most critical for *Xoo* virulence in the Korean strain KXO85. This result is similar to other reports indicating that *xopN*$_{Xcv}$ and *xopN*$_{Xcc}$ mutants show reduced virulence [26,28].

It is worth noting that different Xop effectors from different *Xoo* strains have been reported to be major Xops involved in *Xoo* virulence. Differences in genetic backgrounds of *Xoo* strains and rice cultivars used for virulence assays may explain why different research groups have reported different Xops as major virulence factors. For example, in one study, a mutation in the *xopN* homolog in *Xoo* PXO99^A did not alter disease severity in rice cultivar IR24 that was grown in a growth chamber for 4 weeks [35]. However, it should also be noted that differences in environmental conditions and various rice leaf stages used for inoculation of different *Xoo* strains may also result in different outcomes in virulence assays. In previous studies on *Xoo* PXO99^A and Chinese strain 13751, relatively young rice leaves were used for virulence assays in a growth chamber or a greenhouse [35,43], whereas we used flag leaves grown in a paddy field during the regular rice growing season. Disease severity induced by *Xoo* depends on rice leaf stage [36–39]. These observations correspond well with previous reports that the response to *Xoo* in rice depends on the age of the host [36]. Environmental conditions for growing rice and virulence assays are additional factors that may affect disease severity. It will be of interest to determine whether the *xopN*$_{PXO99}$ mutant of *Xoo* PXO99^A shows differences in virulence assays when the mutant is inoculated into rice flag leaves.

Identification of target proteins of bacterial effectors in their hosts provides a basis for understanding effector functions and their roles in pathogenesis and host defense. XopN$_{Xcv}$ targets a tomato atypical receptor-like kinase1 (TARK1) and four tomato 14-3-3 isoforms (TFT1, TFT3, TFT5, and TFT6) to affect the defense signal mechanism [28]. In *Xoo*, the Xoo1488 of *Xoo* MAFF311018 inhibits OsRLCK185 phosphorylation and the downstream MAPK signaling [31]. Therefore, we postulated that XopN$_{KXO85}$ may interact with known kinases that are involved in signal transduction pathways in rice. However, unlike OsRLCK185 in rice, we found no kinase homologs as XopN$_{KXO85}$ targets but rather two previously unknown rice proteins, OsVOZ2 and OsXNP, were identified based on yeast two-hybrid analysis, pull-down, and BiFC assays.

The AtVOZs were first identified as novel transcription factors in *A. thaliana* [44]. AtVOZs interact with phytochrome B and accelerate flowering time in *A. thaliana* [45]. In the nuclei of *A. thaliana* cells, AtVOZ2 is controlled by light quality in a phytochrome-dependent manner [45]. In addition, AtVOZs are involved in controlling many stress reactions and changing the expression of various stress-related genes, such as those related to drought or freezing responses and pathogens [46]. The genome of the wild-type rice Dongjin has an OsVOZ2 homolog, OsVOZ1, which is also an ortholog of AtVOZ2 and has conserved zinc finger amino acid residues [44]. OsVOZ1 and OsVOZ2 share 60.4% identity (Figure S6). Due to the high degrees of similarity between OsVOZ1 and OsVOZ2, we performed BiFC analysis to determine whether OsVOZ1 is a target protein of XopN$_{KXO85}$. However, there was no evidence of an interaction between XopN$_{KXO85}$ and OsVOZ1 (Figure 2C).

AtVOZ2 interacts with five proteins in *A. thaliana*: phytochrome B (PHY B, At2g18790), guanine nucleotide-binding protein alpha-1 subunit (GP ALPHA1, At2g26300), guanine nucleotide-binding protein subunit beta (AGB1,At4g34460), pirin (PRN, At3g59220), and a hypothetical protein (At4g26410) [45,47]. The most apparent AtVOZ2-dependent phenotype is regulation of flowering period in *A. thaliana* after it interacts with phytochrome B [45]. However, it appears that OsVOZ2 is not involved in determining rice flowering time because we found no noticeable differences in flowering time between wild-type Dongjin and the *OsVOZ2* mutant rice line. Other than our findings indicating that OsVOZ2 is a target of XopN$_{KXO85}$ and is involved in *Xoo* virulence, no other functions have yet been reported in rice.

Another target of XopN$_{KXO85}$ is a putative thiamine synthase, OsXNP, which is present as a single-copy gene in rice. The thiamine synthase gene is related to pathogen-induced defense-responsive protein 8 in Indica rice cultivars. Treatment with thiamine induces callose deposition and hydrogen peroxide accumulation and triggers systemic acquired resistance and transient expression of pathogenesis-related genes against pathogen invasion in rice and several other plants [48,49]. These phenomena are consistent with the observation that thiamine plays important roles in host defense mechanisms against pathogen infection. Therefore, we propose that XopN$_{KXO85}$ interacts with a putative thiamine synthase to hinder thiamine biosynthesis, thereby decreasing the defense of rice against *Xoo* infection. The target proteins of XopN$_{KXO85}$ in rice are completely different from the previously reported targets of XopN$_{Xcv}$. These observations indicate that XopN plays a common role as a virulence factor in *Xcv*, *Xcc*,
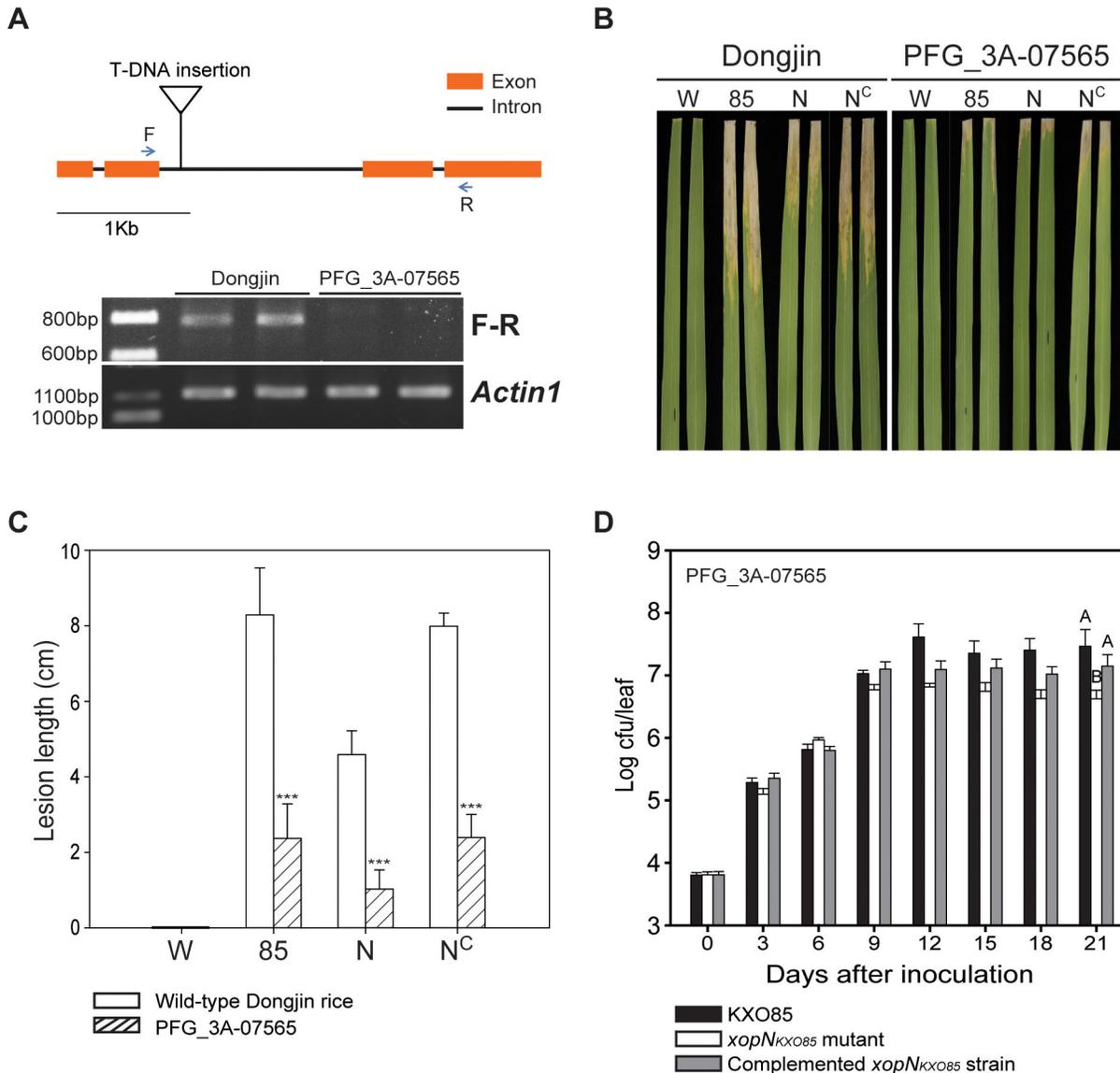
Figure 4. Virulence assay in wild-type Dongjin rice and the OsVOZ2 mutant line PFG_3A-07565. A. Schematic representation of the T-DNA insertion in OsVOZ2 T_7 transgenic rice. *OsVOZ2* consists of four exons (orange boxes) and three introns (line between the orange boxes). The T-DNA was located in the second intron from the translational start site. F and R are the primers used for RT-PCR analysis, which showed the expected size of *OsVOZ2* in wild-type Dongjin but not in the *OsVOZ2* mutant rice PFG_3A-07565. Actin1 was used for normalization of the cDNA quantity. **B**. Virulence assay of the *xopN$_{KXO85}$* mutant in wild-type Dongjin rice and OsVOZ2 mutant rice. W, water; 85, KXO85; N, KXO85 *xopN$_{KXO85}$*::EZ-Tn*5*; and N^C, KXO85 *xopN$_{KXO85}$*::EZ-Tn*5* (pML122G2). Photographs were taken 21 days after inoculation. **C**. Measurement of disease severity in flag leaves of wild-type Dongjin rice (□) and OsVOZ2 mutant rice (▨). W, water; 85, KXO85; N, KXO85 *xopN$_{KXO85}$*::EZ-Tn*5*; and N^C, KXO85 *xopN$_{KXO85}$*::EZ-Tn*5* (pML122G2). Lesion lengths were determined 21 days after inoculation. Vertical error bars indicate the standard deviation (SD). The statistical significance was determined using a two-way ANOVA as compared to wild-type Dongjin rice with the post hoc Tukey HSD test (***, P<0.001). **D**. Growth patterns of the KXO85, *xopN$_{KXO85}$* mutant, and complemented *xopN$_{KXO85}$* mutant in the flag leaves of OsVOZ2 mutant rice (PFG_3A-07565). The data are the average values of three replicates; vertical bars indicate the error ranges (±SD). The bacterial populations were assessed every 3 days after inoculation. Different letters at day 21 indicate significant differences (P<0.05) as determined by a one-way ANOVA (P<0.001) followed by post hoc Tukey HSD analysis.

doi: 10.1371/journal.pone.0073346.g004

and *Xoo* but functions in different ways in monocots and dicots, reflecting the different pathogen response mechanisms that arose during the coevolution of pathogens and their hosts.

In addition to roles of XopN$_{KXO85}$ as a virulence factor, OsVOZ2 is also important for *Xoo* virulence because wild-type KXO85 failed to successfully infect OsVOZ2 mutant rice. This suggests that interactions between XopN$_{KXO85}$ and OsVOZ2 in rice increases susceptibility to *Xoo* infection. That is, *Xoo* produces XopN$_{KXO85}$ as an effector molecule and utilizes the host protein OsVOZ2 for successful infection and increased virulence. Although the functions of OsVOZ2 are not fully understood in the interactions between *Xoo* and rice, it is evident that OsVOZ2 is a key factor in *Xoo* virulence in rice.

Materials and Methods

Ethics Statement

No specific permits were required for these kinds of field studies. This field is owned by the University Farm, College of Agriculture and life Sciences, Seoul National University. This university farm is located in Suwon, which is approximately 40 kilometers south of the main campus of Seoul National University in Seoul, Republic of Korea. The location is not privately-owned or protected in any way. The field studies did not involve endangered or protected species.

Bacterial strains

The bacterial strains and plasmids used in this study are listed in Table S3. All of the *Xoo* strains used were derivatives of the parent strain KXO85 (KACC10331). *Escherichia coli* cells were grown at 37°C in Luria-Bertani (LB) broth or on LB agar plates. The *Xoo* strains were grown at 28°C in PS broth (PSB: peptone 1%, sucrose 1%, sodium L-glutamate 0.1%) or PS agar (PSA) plates. Antibiotics were used at the following concentrations: ampicillin, 100 µg/mL; gentamycin, 20 µg/mL; kanamycin, 50 µg/mL; tetracycline, 10 µg/mL; and spectinomycin, 50 µg/mL for *E. coli* strains and cephalexin 10 µg/mL; gentamycin, 10 µg/mL; tetracycline, 2 µg/mL; and kanamycin, 25 µg/mL for *Xoo* strains.

Transposon insertion and marker-exchange mutagenesis

All recombinant DNA techniques were performed according to standard methods [50]. To generate the *xopN*$_{KXO85}$ mutant, the approximately 3-kb *Bam*HI fragment carrying the *xopN*$_{KXO85}$ gene from BAC clone G2 (Table S3) of *Xoo* KXO85 was cloned into pML122. EZ-Tn*5*<TET-1> was inserted into the coding region of *xopN*$_{KXO85}$ in pML122 by *in vitro* transposition according to the supplier's instructions (Epicentre) yielding pXopN::EZ-Tn*5* (Table S3). pXopN::EZ-Tn*5* was electroporated into *Xoo* KXO85, and the transformed cells were cultured on PSA medium containing tetracycline. The marker-exchanged mutant *Xoo* KXO85 *xopN*$_{KXO85}$::EZ-Tn*5* was isolated and confirmed by Southern hybridization. Transposon insertion and marker-exchange mutagenesis of the other *xop* genes (*xopQ*$_{KXO85}$, *xopX*$_{KXO85}$, *xopP2*$_{KXO85}$, and *xopP1*$_{KXO85}$) were

performed by the same strategy as described above to generate the *xopN*$_{KXO85}$ mutant in *Xoo* KXO85.

Virulence assay

Rice plants of cultivar Dongjin were grown in a paddy field. The *OsVOZ2* mutant rice seeds (PFG_3A-07565; T$_0$ seed) were affirmed by the rice T-DNA Insertion Sequence Database (http://signal.salk.edu/cgi-bin/RiceGE) [41]. The homozygous T$_7$ transgenic mutant line of the *OsVOZ2* mutant rice was obtained and confirmed by RT-PCR analysis. Overnight cultures of *Xoo* cells were adjusted to approximately 1.8×10^8 CFU/mL and inoculated into 3-month-old leaves or fully expanded flag leaves by the scissor clip method [51]. Symptoms were scored by measuring lesion lengths 21 days after inoculation. The growth of *Xoo* cells in plants was determined as described previously [16].

Quantitative real time RT-PCR analysis

The bacterial strains used were cultured in liquid medium XOM2 [52] or PSB for 24 h. Total RNA was isolated from the wild-type strain KXO85 and KXO85 *hrpX*$_{KXO85}$::EZ-Tn*5* using an RNeasy kit (Qiagen) according to the manufacturer's instructions. A total of 1 µg RNA was reverse transcribed into cDNA using M-MLV reverse transcriptase (Promega) for 1 h at 42°C. RT-PCR products from samples were analyzed on agarose gels and the bacterial 16s rRNA was used as a standard. Quantitative real-time RT-PCR (qRT-PCR) was performed using the cDNA and gene-specific primers (Table S4). The transcription levels were determined by Power SYBR Green PCR Master Mix on an Applied Biosystems 7500 Real-Time PCR System (Applied Biosystems). The thermal cycling parameters were: 95°C for 10 min, followed by 40 cycles of 95°C for 30 s and 60°C for 1 min. Expression of 16S rRNA was used to normalize the expression values in each sample, and relative expression values were determined against the average value of wild-type strain KXO85 using the comparative Ct method.

Adenylate cyclase assays

To generate the *xopN-cya* gene fusion protein, the *xopN*$_{KXO85}$ gene was cloned into the *Xba*I and *Xho*I sites of pMLTC to generate pMCXopN (Table S3) followed by transformation into *Xoo* KXO85 and KXO85 *hrpB5*$_{KXO85}$::EZ-Tn*5*. For the assay of adenylate cyclase activity in rice leaf tissues, rice leaves were hand-inoculated with bacterial suspension using a needleless syringe. After 12 h, samples were frozen with liquid nitrogen and homogenized in assay buffer supplied with the cAMP Biotrak Enzyme Immunoassay System (GE Healthcare). The level of cAMP in leaf samples was measured by the cAMP Biotrak Enzyme Immunoassay System according to the manufacturer's directions.

Yeast two-hybrid assay

A Gal4-based system with Gateway technology (Invitrogen) was used for a yeast two-hybrid assay. The *xopN*$_{KXO85}$ gene was amplified by PCR using *Xoo* KXO85 genomic DNA as a template. The PCR primers (Table S5) were flanked with the

attB1 and attB2 sites required for the Gateway cloning system. The PCR product was cloned into pDONR222 by BP recombination to generate the entry clone. Subsequently, the *xopN*$_{KXO85}$ gene was transferred to the yeast destination bait plasmid pDEST32 by LR recombination resulting in pD32XopN (Table S3). To construct a Dongjin cDNA library, cDNA of approximately 0.5–3 kb was cloned into pDONR222 and subsequently into the prey plasmid pDEST22 by LR recombination yielding pD22Lib (Table S3). pD32XopN contains the DNA-binding domain of Gal4 and the leucine selection marker gene *LEU2*. pD22Lib contains the GAL4 transcription activation domain and the tryptophan selection marker gene *TRP1*. All constructs were checked by restriction enzyme analysis and confirmed by DNA sequencing. pD32XopN (bait) and pD22Lib (prey) were co-transformed into yeast strain MaV203 according to the manufacturer's protocol (Invitrogen). The transformants were cultured on synthetic complete (SC) medium lacking leucine (–Leu) and tryptophan (–Trp). After 72 h, colonies were picked and mixed with 100 µL of sterile water, and 10 µL of the cell suspension was spotted onto selection plates to screen for expression of the three reporter genes (*HIS3*, *URA3*, and *lacZ*). Growth of the yeast transformants was assessed on SC–Leu–Trp–His supplemented with 0–50 mM 3-amino-1,2,4-triazole (3AT) as a histidine inhibitor and SC–Leu–Trp–Ura. A change in the blue color of the transformants was monitored in the presence of X-Gal (5-bromo-4-chloro-3-indolyl-β-d-galactopyranoside). To check for autoactivation of the reporter genes, pD32XopN, pD22OsVOZ2, and pD22OsXNP were combined with pDEST32 or pDEST22 and tested for autoactivation activity. We used the controls provided by Invitrogen: S (strong control: pEXP ™32/Krev1 + pEXP ™22/RalGDS-wt), W (weak control: pEXP ™32/Krev1 + pEXP ™22/RalGDS-m1), and A (absent control: pEXP ™32/Krev1 + pEXP ™22/RalGDS-m2). Protein expression was confirmed by immunoblotting using anti-GAL4BD (Clontech) and anti-GAL4AD (Clontech) antibodies. Signals were visualized using an Immun-Star WesternC Kit (Bio-Rad).

Agrobacterium-mediated transient expression

Agrobacterium infiltration into *N. benthamiana* leaves was performed as described previously [28]. Cells of *A. tumefaciens* strain C58C1 (pCH32) [53] were cultured at 28°C for 2 days on LB agar medium containing 50 µg/mL kanamycin and 2.5 µg/mL tetracycline. The recombinant agrobacteria were grown in 10 mL LB liquid medium supplemented with appropriate antibiotics at 28°C and then harvested by centrifugation. The cell pellet was resuspended in buffer (10 mM MES, pH 5.6, 10 mM MgCl$_2$, and 150 µM acetosyringone), adjusted to a final OD$_{600}$ of 0.6, and then incubated for 3 h at room temperature before inoculation. Cells were hand-infiltrated onto *N. benthamiana* leaves using a needleless 1 mL syringe. Inoculated plants were incubated at 26°C in a growth chamber for 1 to 2 days.

In vivo pull-down assay

To generate plasmids for Ni-NTA affinity pull-down assays, pENTR-XopN, pENTR-OsVOZ2, and pENTR-OsXNP were recombined into pGWB8, pGWB12, and pGWB11 by LR recombination yielding pGWB8-XopN, pGWB12-OsVOZ2, and pGWB11-OsXNP, respectively (Table S3). XopN$_{KXO85}$ was tagged with 6× His, OsVOZ2 was tagged with Flag at the N-terminal, and OsXNP was tagged with Flag at the C-terminal. The bacterial suspensions of *A. tumefaciens* coexpressing XopN$_{KXO85}$-6× His/Flag-OsVOZ2 and XopN$_{KXO85}$-6× His/OsXNP-Flag were hand-infiltrated into *N. benthamiana* leaves. At 30 h after infiltration, the leaves were frozen with liquid nitrogen and then macerated in extraction buffer (100 mM sodium phosphate, pH 7.4, 20 mM imidazole, and 0.15% Triton X-100). Homogenized samples were mixed for 1 h at 4°C and centrifuged for 15 min at 17000 × *g* at 4°C. The soluble extracts were incubated with 30 µL 50% slurry of Ni-NTA Superflow Agarose (Qiagen). Ni-NTA agarose was retrieved by centrifugation and washed three times with extraction buffer, and proteins were eluted with 8 M urea sample buffer followed by Western blotting analysis using anti-6× His (Qiagen) and anti-FLAG (Sigma) antibodies. Signals were visualized using detection solution (Immun-Star WesternC Kit; Bio-Rad).

BiFC

The coding regions of *xopN*$_{KXO85}$, *OsVOZ2*, *OsXNP*, and *OsVOZ1* were amplified by PCR using proofreading DNA polymerase and appropriate primers (Table S6) and cloned into the Gateway entry vector pENTR D TOPO (Invitrogen) yielding pENTR-XopN, pENTR-OsVOZ2, pENTR-OsXNP, and pENTR-OsVOZ1, respectively. pENTR-XopN, pENTR-OsVOZ2, pENTR-OsXNP, and pENTR-OsVOZ1 were recombined into the Gateway binary BiFC vectors pDEST-SCYNE(R)^{GW} and pDEST-SCYCE(R)^{GW} using LR recombinase according to the manufacturer's instructions (Invitrogen) yielding pSCYNE-XopN, pSCYCE-OsVOZ2, pSCYCE-OsXNP, and pSCYCE-OsVOZ1, respectively (Table S3). The constructs were confirmed by DNA sequencing and transformed into *A. tumefaciens* C58C1 (pCH32) for transient expression in *N. benthamiana* as described above. SCFP signals were detected using a confocal laser scanning microscope (Leica Microsystems) 26 h after infiltration.

Localization of OsVOZ2, OsXNP, and XopN$_{KXO85}$

The *OsVOZ2*, *OsXNP*, and *xopN*$_{KXO85}$ genes in pENTR D TOPO were cloned into the destination vector p2GWF7 to create a C-terminal GFP fusion [54] using the Gateway LR recombinase (Invitrogen). The constructs were introduced into maize mesophyll protoplasts by polyethylene glycol–calcium-mediated transformation [55,56]. The protoplasts were examined after incubation for 12–24 h. OsABF1-RFP was used as a nuclear marker [57].

Microscopy

We used confocal laser scanning microscopes (SCFP: TCS SP5; Leica Microsystems; GFP: LSM510 META; Carl Zeiss) to detect the SCFP and GFP signals. The excitation and emission wavelengths were SCFP (458 nm and 465–480 nm, respectively) and GFP (488 nm and 500–525 nm, respectively).

Statistical analysis

JMP® 10 software (SAS Institute) was used for statistical analysis. Statistical significance was determined by a one-way or a two-way ANOVA with Tukey HSD post-test.

Supporting Information

Figure S1. Genetic organization of five *xop* genes and EZ-Tn*5* insertion positions in the *Xoo* KXO85 genome. The vertical bar with black open triangle indicates the position of the EZ-Tn*5* insertion. Arabic numerals on the left and right sides indicate the base position in the *Xoo* KXO85 genome. (DOC)

Figure S2. *XopN*$_{KXO85}$ expression is regulated by HrpX$_{KXO85}$ in *Xoo* KXO85. A. Expression profiles of *XopN*$_{KXO85}$ regulated by HrpX$_{KXO85}$ based on RT-PCR (left panel) and qRT-PCR (right panel) analyses. The 16S rRNA gene of KXO85 was used for normalization of the cDNA quantity and expression value. WT, *Xoo* KXO85; X, *Xoo* KXO85 *hrpX*$_{KXO85}$::EZ-Tn5; PSB, bacterial strains were incubated in PSB (1% peptone, 1% sucrose, and 0.1% sodium L-glutamate); XOM2, bacterial strains were incubated in *hrp*-inducing medium XOM2. Vertical error bars indicate the standard deviation. **B**. The PIP box (TTCGG-N$_{15}$-TTCTG) is located near *XopN*$_{KXO85}$ in the KXO85 genome. (DOC)

Figure S3. Genetic map of the *hrpB5*$_{KXO85}$ mutant and cAMP measurement in rice leaves. A. The vertical bar with a black open triangle indicates the position of the EZ-Tn*5* insertion in *hrpB5*$_{KXO85}$ in the KXO85 genome. The numbers on the left and right sides indicate the base positions in the KXO85 genome. **B**. Levels of cAMP in rice leaves. WT, KXO85; B5, KXO85 *hrpB5*$_{KXO85}$::EZ-Tn5; N, KXO85 (pMC*xopN*); B5-N, KXO85 *hrpB5*$_{KXO85}$::EZ-Tn*5* (pMC*xopN*); TC, KXO85 (pMLTC)-vector control; B5-TC, KXO85 *hrpB5*$_{KXO85}$::EZ-Tn*5* (pMLTC)-vector control; and W, water. For the cAMP assays, each data point represents the average of three replicate samples with error bars indicating the standard deviation. (DOC)

Figure S4. Self-activation test and Western blot analysis showing expression of the yeast plasmid constructs in yeast two-hybrid screening. A. Self-activation tests were conducted using pD32XopN + pDEST22, pDEST32 + pD22OsVOZ2, pDEST32 + pD22OsXNP, and pDEST32 + pDEST22. **B**. Total proteins were extracted from the indicated yeast strains. Anti-GAL4BD and anti-GAL4AD antibodies were used for immunoblotting. M, size marker; 1, pD32XopN and pD22OsVOZ2; 2, pD32XopN and pD22OsXNP; and 3,

pDEST32 and pDEST22. The expected molecular weights of the proteins were as follows: GAL4BD-XopN$_{KXO85}$ = 94. 4 kDa; GAL4AD-OsVOZ2 = 84.8 kDa; GAL4AD-OsXNP = 53.2 kDa; GAL4BD: 18. 4 kDa; and GAL4AD: 14.9 kDa. The arrow (◄) indicates the position of expressed protein. (DOC)

Figure S5. The amino acid sequence alignment of *A. thaliana* VOZ2 and OsVOZ2 using the ClustalW2 multiple alignment program. (DOC)

Figure S6. The amino acid sequence alignment of OsVOZ1 and OsVOZ2 using the ClustalW2 multiple alignment program. The red box represents conserved residues possibly forming a functional zinc-coordinating motif. (DOC)

Table S1. Characteristics of five predicted *xop* genes from *Xoo* KXO85. (DOC)

Table S2. Identification of OsVOZ2 and OsXNP. (DOC)

Table S3. Bacterial strains and plasmids. (DOC)

Table S4. Primers used for qRT–PCR of *xopN*$_{KXO85}$. (DOC)

Table S5. Primers used for yeast two-hybrid system. (DOC)

Table S6. Primers used for BiFC, localization, and *in vivo* pull-down assay. (DOC)

Author Contributions

Conceived and designed the experiments: IH J-SJ JSM. Performed the experiments: HC C-YK. Analyzed the data: HC C-YK IH J-SJ JSM. Contributed reagents/materials/analysis tools: B-ML. Wrote the manuscript: HC J-SJ IH.

References

1. Lee B-M, Park Y-J, Park D-S, Kang H-W, Kim J-G et al. (2005) The genome sequence of *Xanthomonas oryzae* pathovar *oryzae* KACC10331, the bacterial blight pathogen of rice. Nucleic Acids Res 33: 577-586. doi:10.1093/nar/gki591. PubMed: 15673718.

2. Büttner D, He SY (2009) Type III protein secretion in plant pathogenic bacteria. Plant Physiol 150: 1656-1664. doi:10.1104/pp.109.139089. PubMed: 19458111.

3. Büttner D, Bonas U (2002) Port of entry-the type III secretion translocon. Trends Microbiol 10: 186-192. doi:10.1016/S0966-842X(02)02331-4. PubMed: 11912026.

4. Crabill E, Karpisek A, Alfano JR (2012) The *Pseudomonas syringae* HrpJ protein controls the secretion of type III translocator proteins and has a virulence role inside plant cells. Mol Microbiol 85: 225-238. doi:10.1111/j.1365-2958.2012.08097.x. PubMed: 22607547.

5. Galán JE, Collmer A (1999) Type III secretion machines: bacterial devices for protein delivery into host cells. Science 284: 1322-1328. doi:10.1126/science.284.5418.1322. PubMed: 10334981.

6. Ghosh P (2004) Process of protein transport by the type III secretion system. Microbiol Mol Biol Rev 68: 771-795. doi:10.1128/MMBR.68.4.771-795.2004. PubMed: 15590783.

7. Alfano JR, Collmer A (2004) Type III secretion system effector proteins: Double agents in bacterial disease and plant defense. Annu Rev Phytopathol 42: 385-414. doi:10.1146/annurev.phyto.42.040103.110731. PubMed: 15283671.

8. Boureau T, Siamer S, Perino C, Gaubert S, Patrit O et al. (2011) The HrpN effector of *Erwinia amylovora*, which is involved in type III translocation, contributes directly or indirectly to callose elicitation on apple leaves. Mol Plant Microbe Interact 24: 577-584. doi:10.1094/MPMI-09-10-0212. PubMed: 21463207.

9. Göhre V, Robatzek S (2008) Breaking the barriers: Microbial effector molecules subvert plant immunity. Annu Rev Phytopathol 46: 189-215. doi:10.1146/annurev.phyto.46.120407.110050. PubMed: 18422429.

10. Meyer D, Cunnac S, Guéneron M, Declercq C, Van Gijsegem F et al. (2006) PopF1 and PopF2, two proteins secreted by the type III protein secretion system of *Ralstonia solanacearum*, are translocators belonging to the HrpF/NopX family. J Bacteriol 188: 4903-4917. doi:10.1128/JB.00180-06. PubMed: 16788199.

11. Mudgett MB (2005) New insights to the function of phytopathogenic bacterial type III effectors in plants. Annu Rev Plant Biol 56: 509-531. doi:10.1146/annurev.arplant.56.032604.144218. PubMed: 15862106.

12. Petnicki-Ocwieja T, van Dijk K, Alfano JR (2005) The *hrpK* operon of *Pseudomonas syringae* pv. *tomato* DC3000 encodes two proteins secreted by the type III (Hrp) protein secretion system: HopB1 and HrpK, a putative type III translocator. J Bacteriol 187: 649-663. doi:10.1128/JB.187.2.649-663.2005. PubMed: 15629936.

13. Furutani A, Takaoka M, Sanada H, Noguchi Y, Oku T et al. (2009) Identification of novel type III secretion effectors in *Xanthomonas oryzae* pv. *oryzae*. Mol Plant Microbe Interact 22: 96-106. doi:10.1094/MPMI-22-1-0096. PubMed: 19061406.

14. Scholze H, Boch J (2011) TAL effectors are remote controls for gene activation. Curr Opin Microbiol 14: 47-53. doi:10.1016/j.mib.2010.12.001. PubMed: 21215685.

15. White FF, Potnis N, Jones JB, Koebnik R (2009) The type III effectors of *Xanthomonas*. Mol Plant Pathol 10: 749-766. doi:10.1111/j.1364-3703.2009.00590.x. PubMed: 19849782.

16. Sugio A, Yang B, White FF (2005) Characterization of the *hrpF* pathogenicity peninsula of *Xanthomonas oryzae* pv. *oryzae*. Mol Plant Microbe Interact 18: 546-554. doi:10.1094/MPMI-18-0546. PubMed: 15986924.

17. Zhu W, Magbanua MM, White FF (2000) Identification of Two Novel *hrp*-Associated Genes in the *hrp* Gene Cluster of *Xanthomonas oryzae* pv. *oryzae*. J Bacteriol 182: 1844-1853. doi:10.1128/JB.182.7.1844-1853.2000. PubMed: 10714988.

18. Bai J, Choi SH, Ponciano G, Leung H, Leach JE (2000) *Xanthomonas oryzae* pv. *oryzae* avirulence genes contribute differently and specifically to pathogen aggressiveness. Mol Plant Microbe Interact 13: 1322-1329. doi:10.1094/MPMI.2000.13.12.1322. PubMed: 11106024.

19. Boch J, Bonas U (2010) *Xanthomonas* AvrBs3 family-type III effectors: discovery and unction. Annu Rev Phytopathol 48: 419-436. doi:10.1146/annurev-phyto-080508-081936. PubMed: 19400638.

20. Bogdanove AJ, Schornack S, Lahaye T (2010) TAL effectors: finding plant genes for disease and defense. Curr Opin Plant Biol 13: 394-401. doi:10.1016/j.pbi.2010.04.010. PubMed: 20570209.

21. Hwang IS, Kim NH, Choi DS, Hwang BK (2012) Overexpression of *Xanthomonas campestris* pv. *vesicatoria* effector AvrBsT in Arabidopsis triggers plant cell death, disease and defense responses. Planta 236: 1191-1204. doi:10.1007/s00425-012-1672-4. PubMed: 22678032.

22. Roden JA, Eardley L, Hotson A, Cao Y, Mudgett MB (2004) Characterization of the *Xanthomonas* AvrXv4 effector, a SUMO protease translocated into plant cells. Mol Plant Microbe Interact 17: 633-643. doi:10.1094/MPMI.2004.17.6.633. PubMed: 15195946.

23. Yu Y, Streubel J, Balzergue S, Champion A, Boch J, Koebnik R et al. (2011) Colonization of rice leaf blades by an African strain of *Xanthomonas oryzae* pv. *oryzae* depends on a new a TAL effector that induces the rice nodulin-3 Os11N3 gene. Mol Plant Microbe Interact 24: 1102-1113. doi:10.1094/MPMI-11-10-0254. PubMed: 21679014.

24. Metz M, Dahlbeck D, Morales CQ, Sady BA, Clark ET et al. (2005) The conserved *Xanthomonas campestris* pv. *vesicatoria* effector protein XopX is a virulence factor and suppresses host defense in *Nicotiana benthamiana*. Plant J 41: 801-814. doi:10.1111/j.1365-313X.2005.02338.x. PubMed: 15743446.

25. Kim J-G, Taylor KW, Hotson A, Keegan M, Schmelz EA et al. (2008) XopD SUMO protease affects host transcription, promotes pathogen growth, and delays symptom development in *Xanthomonas*-infected tomato leaves. Plant Cell 20: 1915-1929. doi:10.1105/tpc.108.058529. PubMed: 18664616.

26. Jiang B-L, He Y-Q, Cen W-J, Wei H-Y, Jiang G-F et al. (2008) The type III secretion effector XopXccN of *Xanthomonas campestris* pv. *campestris* is required for full virulence. Res Microbiol 159: 216-220. doi:10.1016/j.resmic.2007.12.004. PubMed: 18281198.

27. Roden JA, Belt B, Ross JB, Tachibana T, Vargas J et al. (2004) A genetic screen to isolate type III effectors translocated into pepper cells during *Xanthomonas* infection. Proc Natl Acad Sci U S A 101: 16624-16629. doi:10.1073/pnas.0407383101. PubMed: 15545602.

28. Kim J-G, Li X, Roden JA, Taylor KW, Aakre CD et al. (2009) Xanthomonas T3S effector XopN suppresses PAMP-triggered immunity and interacts with a tomato atypical receptor-like kinase and TFT1. Plant Cell 21: 1305-1323.

29. Canonne J, Marino D, Jauneau A, Pouzet C, Brière C et al. (2011) The *Xanthomonas* type III effector XopD targets the *Arabidopsis* transcription factor MYB30 to suppress plant defense. Plant Cell 23: 3498-3511. doi:10.1105/tpc.111.088815. PubMed: 21917550.

30. Kim J-G, Stork W, Mudgett MB (2013) *Xanthomonas* type III effector XopD desumoylates tomato transcription factor SlERF4 to suppress ethylene responses and promote pathogen growth. Cell Host Microbe 13: 143-154. doi:10.1016/j.chom.2013.01.006. PubMed: 23414755.

31. Yamaguchi K, Yamada K, Ishikawa K, Yoshimura S, Hayashi N et al. (2013) A receptor-like cytoplasmic kinase targeted by a plant pathogen effector is directly phosphorylated by the chitin receptor and mediates rice immunity. Cell Host Microbe 13: 347-357. doi:10.1016/j.chom.2013.02.007. PubMed: 23498959.

32. Gu K, Yang B, Tian D, Wu L, Wang D et al. (2005) R gene expression induced by a type-III effector triggers disease resistance in rice. Nature 435: 1122-1125. doi:10.1038/nature03630. PubMed: 15973413.

33. Verdier V, Triplett LR, Hummel AW, Corral R, Cernadas RA et al. (2012) Transcription activator-like (TAL) effectors targeting OsSWEET genes enhance virulence on diverse rice (*Oryza sativa*) varieties when expressed individually in a TAL effector-deficient strain of *Xanthomonas oryzae*. New Phytol 196: 1197-1207. doi:10.1111/j.1469-8137.2012.04367.x. PubMed: 23078195.

34. Römer P, Recht S, Strauss T, Elsaesser J, Schornack S et al. (2010) Promoter elements of rice susceptibility genes are bound and activated by specific TAL effectors from the bacterial blight pathogen, *Xanthomonas oryzae* pv. *oryzae*. New Phytol 187: 1048-1057. doi:10.1111/j.1469-8137.2010.03217.x. PubMed: 20345643.

35. Song C, Yang B (2010) Mutagenesis of 18 type III effectors reveals virulence function of XopZ$_{PXO99}$ in *Xanthomonas oryzae* pv. *oryzae*. Mol Plant Microbe Interact 23: 893-902. doi:10.1094/MPMI-23-7-0893. PubMed: 20521952.

36. Goel RK, Gupta AK (1990) Host age in relation to resistance in rice to bacterial blight caused by *Xanthomonas campestris* pv. *oryzae*. Trop Agric 67: 368-370.

37. Mew TW (1987) Current status and future prospects of research on bacterial blight of rice. Annu Rev Phytopathol 25: 359-382. doi:10.1146/annurev.py.25.090187.002043.

38. Sun X, Cao Y, Yang Z, Xu C, Li X et al. (2004) Xa26, a gene conferring resistance to Xanthomonas oryzae pv. oryzae in rice, encodes an LRR receptor kinase-like protein. Plant J 37: 517-527.

39. Zhang Q, Mew TW (1985) Adult-plant resistance of rice cultivars to bacterial blight. Plant Dis 69: 896-898.

40. Gehl C, Waadt R, Kudla J, Mendel R-R, Hänsch R (2009) New gateway vectors for high throughput analyses of protein-protein interactions by bimolecular fluorescence complementation. Mol Plants 2: 1051-1058. doi:10.1093/mp/ssp040. PubMed: 19825679.

41. Jeong DH, An S, Park S, Kang HG, Park GG et al. (2006) Generation of a flanking sequence-tag database for activation tagging lines in japonica rice. Plant J 45: 123-132. doi:10.1111/j.1365-313X.2005.02610.x. PubMed: 16367959.

42. Akimoto-Tomiyama C, Furutani A, Tsuge S, Washington EJ, Nishizawa Y et al. (2012) XopR, a type III effector secreted by *Xanthomonas oryzae* pv. *oryzae*, suppresses microbe-associated molecular pattern-triggered immunity in *Arabidopsis thaliana*. Mol Plant Microbe Interact 25: 505-514. doi:10.1094/MPMI-06-11-0167. PubMed: 22204644.

43. Zhao S, Mo WL, Wu F, Tang W, Tang JL et al. (2013) Identification of non-TAL effectors in *Xanthomonas oryzae* pv. *oryzae* Chinese strain 13751 and analysis of their role in the bacterial virulence. World J Microbiol Biotechnol 29: 733-744. doi:10.1007/s11274-012-1229-5. PubMed: 23296915.

44. Mitsuda N, Hisabori T, Takeyasu K, Sato MH (2004) VOZ; Isolation and characterization of novel vascular plant transcription factors with a one-zinc finger from *Arabidopsis thaliana*. Plant Cell Physiol 45: 845-854. doi:10.1093/pcp/pch101. PubMed: 15295067.

45. Yasui Y, Mukougawa K, Uemoto M, Yokofuji A, Suzuri R et al. (2012) The phytochrome-interacting VASCULAR PLANT ONE-ZINC FINGER1 and VOZ2 redundantly regulate flowering in Arabidopsis. Plant Cell 24: 3248-3263. doi:10.1105/tpc.112.101915. PubMed: 22904146.

46. Nakai Y, Nakahira Y, Sumida H, Takebayashi K, Nagasawa Y et al. (2013) Vascular plant one-zinc-finger protein 1/2 transcription factors regulate abiotic and biotic stress responses in Arabidopsis. Plant J 73: 761-775. doi:10.1111/tpj.12069. PubMed: 23167462.

47. Klopffleisch K, Phan N, Augustin K, Bayne RS, Booker KS et al. (2011) Arabidopsis G-protein interactome reveals connections to cell wall carbohydrates and morphogenesis. Mol Syst Biol 7: 532. PubMed: 21952135.

48. Ahn I-P, Kim S, Lee Y-H (2005) Vitamin B1 functions as an activator of plant disease resistance. Plant Physiol 138: 1505-1515. doi:10.1104/pp.104.058693. PubMed: 15980201.

49. Ahn I-P, Kim S, Lee Y-H, Suh S-C (2007) Vitamin B1-induced priming is dependent on hydrogen peroxide and the NPR1 gene in Arabidopsis. Plant Physiol 143: 838-848. PubMed: 17158583.

50. Sambrook J, Fritsch EF, Maniatis T (1997) Molecular cloning: A laboratory manual. Cold Spring Harbor, NY, USA: Cold Spring Harbor Laboratory Press.

51. Kauffman HE, Reddy APK, Hsieh SPY, Merca SD (1973) An improved technique for evaluating resistance of rice varieties to *Xanthomonas oryzae*. Plant Dis Rep 57: 537-541.

52. Tsuge S, Furutani A, Fukunaka R, Oku T, Tsuno K et al. (2002) Expression of *Xanthomonas oryzae* pv. *oryzae hrp* genes in XOM2, a novel synthetic medium. J Gen Plant Pathol 68: 363-371. doi:10.1007/PL00013104.

53. Mudgett MB, Chesnokova O, Dahlbeck D, Clark ET, Rossier O et al. (2000) Molecular signals required for type III secretion and translocation of the *Xanthomonas campestris* AvrBs2 protein to pepper plants. Proc Natl Acad Sci U S A 97: 13324-13329. doi:10.1073/pnas.230450797. PubMed: 11078519.

54. Karimi M, Inzé D, Depicker A (2002) Gateway vectors for *Agrobacterium*-mediated plant transformation. Trends Plant Sci 7: 193-195. doi:10.1016/S1360-1385(02)02251-3. PubMed: 11992820.

55. Hwang I, Sheen J (2001) Two-component circuitry in Arabidopsis cytokinin signal transduction. Nature 413: 383-389. doi:10.1038/35096500. PubMed: 11574878.

56. Cho JI, Ryoo N, Eom JS, Lee DW, Kim HB et al. (2009) Role of the rice hexokinases OsHXK5 and OsHXK6 as glucose sensors. Plant Physiol 149: 745-759. PubMed: 19010999.

57. Hossain MA, Cho JI, Han M, Ahn CH, Jeon JS et al. (2010) The ABRE-binding bZIP transcription factor OsABF2 is a positive regulator of abiotic stress and ABA signaling in rice. J Plant Physiol 167: 1512-1520. doi:10.1016/j.jplph.2010.05.008. PubMed: 20576316.